Propagation & Imaging Through the Atmosphere IV

Vol. 4125

PROCEEDINGS OF SPIE
SPIE—The International Society for Optical Engineering

Propagation and Imaging through the Atmosphere IV

Michael C. Roggemann
Chair/Editor

3 August 2000
San Diego, USA

Sponsored and Published by
SPIE—The International Society for Optical Engineering

Cooperating Organization
The Remote Sensing Society

SPIE P PROCEEDINGS SERIES

Volume 4125

Please use the following format to cite material from this book:

Author(s), "Title of paper," in *Propagation and Imaging through the Atmosphere IV*, Michael C. Roggemann, Editor, Proceedings of SPIE Vol. 4125, page numbers (2000).

ISSN 0277-786X
ISBN 0-8194-3770-0

Published by
SPIE—The International Society for Optical Engineering
P.O. Box 10, Bellingham, Washington 98227-0010 USA
Telephone 1 360/676-3290 (Pacific Time) • Fax 1 360/647-1445
http://www.spie.org/

Printed in the United States of America.

Conference Committee

Conference Chair

Michael C. Roggemann, Michigan Technological University (USA)

Cochair

Julian C. Christou, University of Oxford (UK)

Program Committee

Timothy J. Kane, The Pennsylvania State University (USA)
Richard G. Paxman, Veridian-ERIM International, Inc. (USA)
Byron M. Welsh, Mission Research Corporation (USA)

Session Chairs

1 Measurements of Turbulence and Turbulence Effects
Michael C. Roggemann, Michigan Technological University (USA)

2 Analysis and Prediction of Turbulence Effects
Bradley R. Stone, Mission Research Corporation (USA)

3 Post-Detection Processing of Images Corrupted by Atmospheric Effects
Richard G. Paxman, Veridian-ERIM International, Inc. (USA)

4 Aerosol Effects
Michael C. Roggemann, Michigan Technological University (USA)

Contents

Does the Detailed Turbulence Profile Matter?

[a]D. Washburn and R. Butts
[a]Air Force Research Laboratory, Directed Energy Directorate, Kirtland AFB, NM 87117-5776

ABSTRACT

The profile of atmospheric turbulence strength along a laser propagation or imaging path is thought to significantly influence performance. We use wave optics simulation to evaluate performance under random variations of turbulence profiles along a 50-km propagation path. Performance is given by power in the bucket (PIB) strehl in a λ/D bucket. For a point source and under the conditions we investigated, we conclude that, in addition to the Rytov parameter, knowledge of r_0 can significantly improve performance prediction.

1. INTRODUCTION

Our goal is to use wave optics simulation to evaluate performance, given by PIB strehl, under random variations of turbulence profiles along the path. The random variations are taken so that the Rytov parameter, *R*, is held fixed. However the random profiles give rise to different values of r_0 and θ_0. We investigate the correlations between r_0 and PIB strehl for fixed Rytov values. For this study λ=1e-6 m, D=0.75 m and the propagation distance was approximately 50-km. We computed both the on axis strehl and the power in the bucket strehl for a λ / D sized bucket. Since the results were very similar for both performance measures, we report only the results for the power in the bucket strehl.

2. THE ATMOSPHERIC MODEL AND PROFILE GENERATION

Our nominal turbulence profile assumed a constant C_n^2 along the propagation path. In the simulation we modeled turbulence by 10 phase screens. The screens were placed at ranges, in meters from the transmitter, as given in r below:

$$r = [400,\ 4025,\ 10475,\ 16925,\ 23375,\ 29825,\ 36275,\ 42725,\ 49175,\ 52500]. \tag{1}$$

Nominal profile strengths were varied to yield Rytov parameters given below:

$$Rytov = 0.125,\ 0.25,\ 0.50,\ 0.75,\ \text{and}\ 1.00.$$

To begin, we discretize the Rytov parameter integral about the phase screen locations specified above.

$$Rytov = 0.563k^{7/6}L^{5/6}\int_0^L dz\, C_n^2(z)\left[\frac{z}{L}\left(1-\frac{z}{L}\right)\right]^{5/6} = 0.563k^{7/6}L^{5/6}C_0\left[\sum_1^{10}\beta_i X_i\right] \tag{2}$$

$$\text{Where: } X_i = \int_{r_i}^{r_{i+1}} dz\left[\frac{z}{L}\left(1-\frac{z}{L}\right)\right]^{5/6}$$

The β_i s are inserted to provide the source of randomness as described below. Since Eq. (2) is linear in the β_i s, we can express it as matrix equation:

$$\left[\sigma_\chi^2\right] = C_0 \mathbf{A}\beta \qquad with\ \ \mathbf{A}\ \ 1X10 \tag{3}$$

Where:

$$\beta = [\beta_1 \quad \beta_2 \quad \ldots \quad \beta_{10}]^T$$

Note that for the nominal turbulence profile, we have

$$\beta = \beta_0 = [1 \quad 1 \quad 1 \quad 1 \quad 1 \quad 1 \quad 1 \quad 1 \quad 1 \quad 1]^T$$

For $C_0 = 4.8465\times10^{-17}\ \text{m}^{-2/3}\beta_0$ we have $rytov = .25$ and $r_0 = 9.72965$ cm. By varying C_0 we can vary the Rytov parameter – henceforth-just Rytov. Note that the nominal r_0 and θ_0 follow from the choice of C_0, as shown in Figure 1. However, as noted, when we vary the profiles holding Rytov fixed, r_0 and θ_0 will vary about the nominal.

Propagation and Imaging through the Atmosphere IV, Michael C. Roggemann, Editor,
Proceedings of SPIE Vol. 4125 (2000) © 2000 SPIE · 0277-786X/00/$15.00

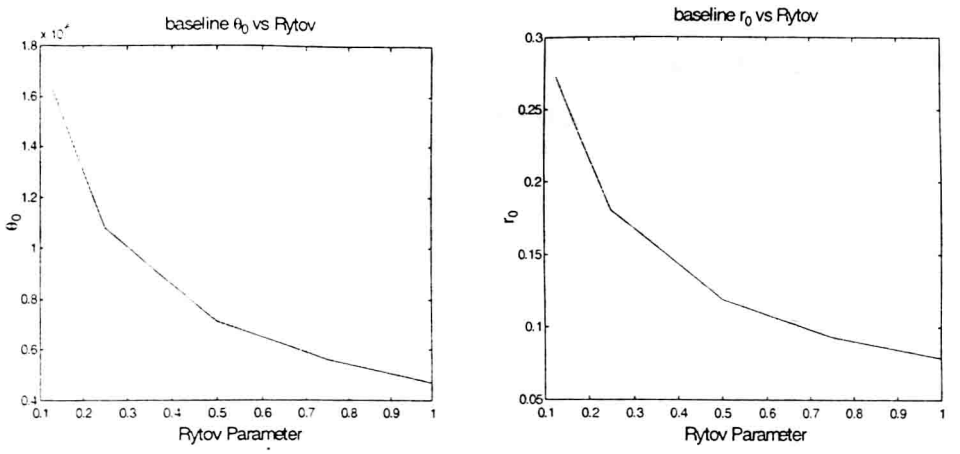

Figure 1 - r_0 and θ_0 versus Rytov

Since **A** has rank 1, it has a null space of dimension 9. We can add any vector in the null space of **A** and still maintain the selected Rytov. A spanning set for the null space of **A** is shown in Figure 2.

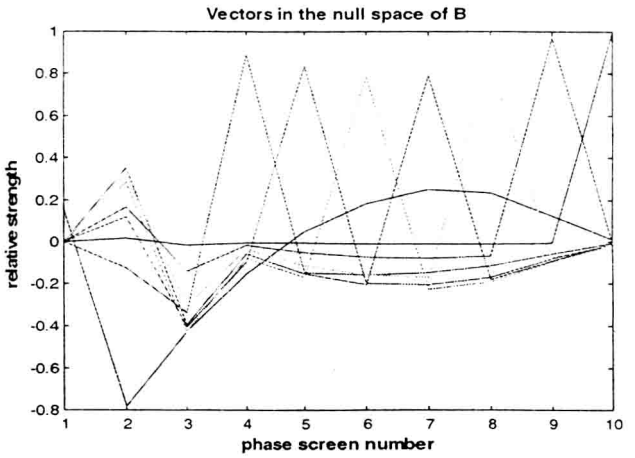

Figure 2 – Null Space Vectors of B

Notice that the null space vectors all have negative components, since all elements of **A** are positive. Thus, if we add a vector in the null space to β_0, we may get a profile that is negative over part of the path and therefore does not correspond to a real C_n^2 profile. In the following we guard against this. We generate a set of profiles satisfying Equation (3) by adding a random linear combination of null space basis vectors of **A** to β_0 to get a new profile. The coefficients of the null space vectors are generated as zero mean Gaussian random numbers with sigma = 4. If a set of random numbers yields a screen strength that is negative, it is discarded and a new set of random numbers generated. For example, to get 50 profiles with no negative values from a population with σ = 4 requires about 1,750,000 random realizations. A set of profiles generated by this procedure is given in Figure 3. Clearly a wide range of turbulence profiles yield the same Rytov.

3. RESULTS

The question we seek to answer is does knowledge of r_0, in addition to Rytov, help improve our performance estimates? To answer this question, we performed a simulation in which phase screens were generated in accordance with the scheme described above.

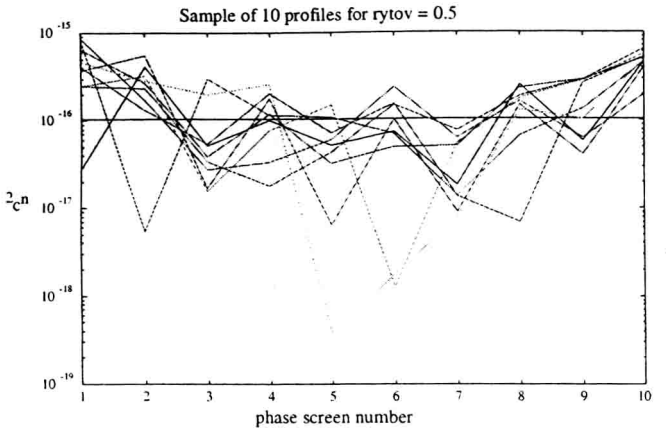

Figure 3 – 10 Random Profiles

In particular, we propagated a point source from the transmitter to the receiver through various atmospheric realizations and used this source to drive the adaptive optics and tracking system. After the control system converged we propagated a scoring beam back to the transmitter and calculated strehls. Thus the results are for an equivalent infinite bandwidth controller.

We calculated statistics for profile strengths with Rytov parameters of 0.125, 0.25, 0.50, 0.75, and 1.00.
For each case we simulated the nominal profile plus fifty random profiles with the same Rytov value. For each profile we did ten random phase screen realizations. Thus we had 510 realizations for each Rytov value. We also calculated 510 random realizations with the nominal profile for comparison with the 510 realizations generated by doing ten realizations each for the 51 different profiles. We calculated both point Strehls and power in the bucket Strehls. Since there was very little difference between the point Strehl and the power in the bucket Strehl, we only show the results for the latter. We also calculated r_0 and θ_0 for each profile. Note that r_0 and θ_0 vary with the profile but do not change with the random realizations of that profile.

Figure 4 shows the spread in Strehls for each of the ten random realizations drawn from each of the 51 atmospheric profiles for Rytov = 0.5. The mean for each set of ten realizations is depicted by a * at the center of a vertical line which spans $\pm\ \sigma$ for that set of ten realizations.

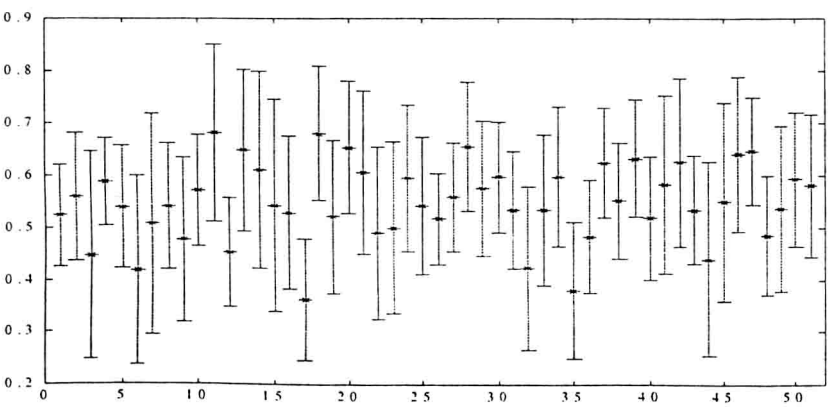

Figure 4 - Profiles averaged ten at a time

Figure 5 shows the means for each set of ten cases, for each of the Rytov values. The * are for the baseline case taken 10 realizations at a time. The solid lines represent the means of ten realizations, but this time changing profiles every ten. The solid straight line through the Rytov = 0.50 data is the overall mean of the Rytov = 0.50 data. Figure 6a indicates that the overall means for all 510 realizations are about the same, whether we are dealing with the baseline profile (*) or whether we are changing profiles (solid line). Figure 6b shows that the standard deviations are in general higher for the case where we are changing profiles, but not significantly so.

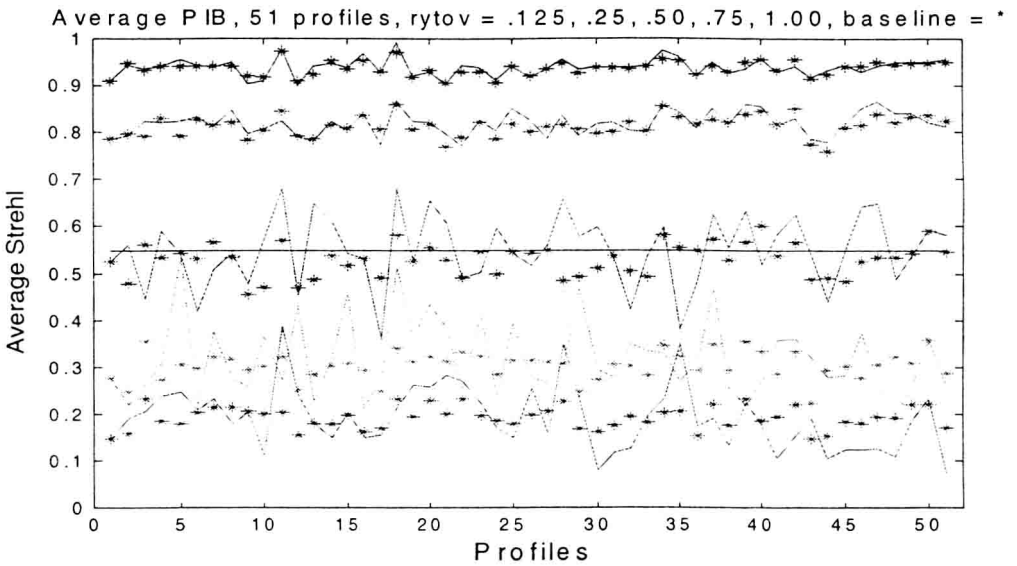

Figure 5 - Average (by tens) PIB for All Cases. The stars (*) represent the baseline profile with the random draws taken 10 at a time. The solid line represents 10 random draws for each of 51 different profiles.

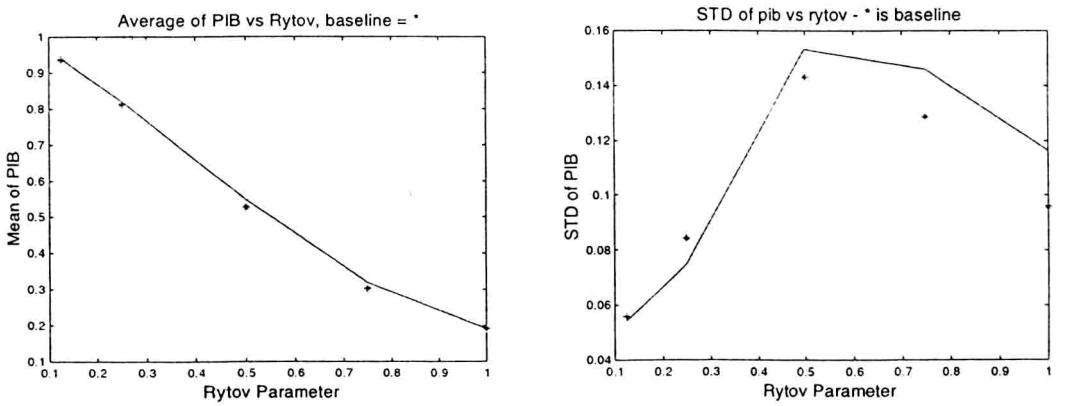

Figure 6 - Mean and standard deviation for all 510 cases for each Rytov value. The stars (*) are for 510 cases for the baseline profile. The solid line is for 510 cases where the profile changes every 10 realizations.

Figure 7 presents a scatter plot of PIB versus r_0 for each of the Rytov values. The highest groupings are for the lowest Rytov. The higher Rytov groupings tend to run together at the bottom left of the chart. However the regression lines are clear.

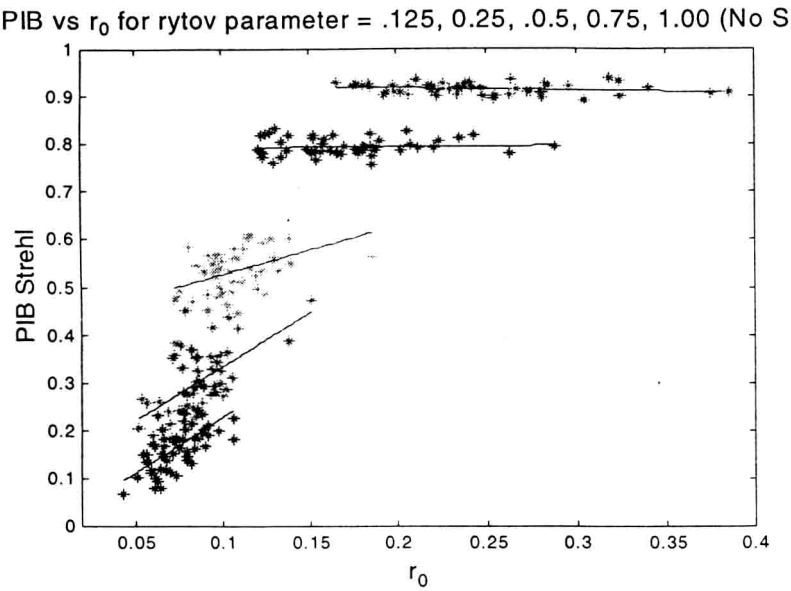

Figure 7: PIB vs r_0 for each of the Rytov cases. Highest groupings are for the lowest Rytov. Solid lines are regression lines through the Rytov groupings

Figure 8 presents the correlation coefficient for PIB vs. r_0. As Rytov increases, the correlation increases. This implies that knowledge of r_0 can improve performance prediction when the turbulence is strong, but has little to offer when the turbulence is weak.

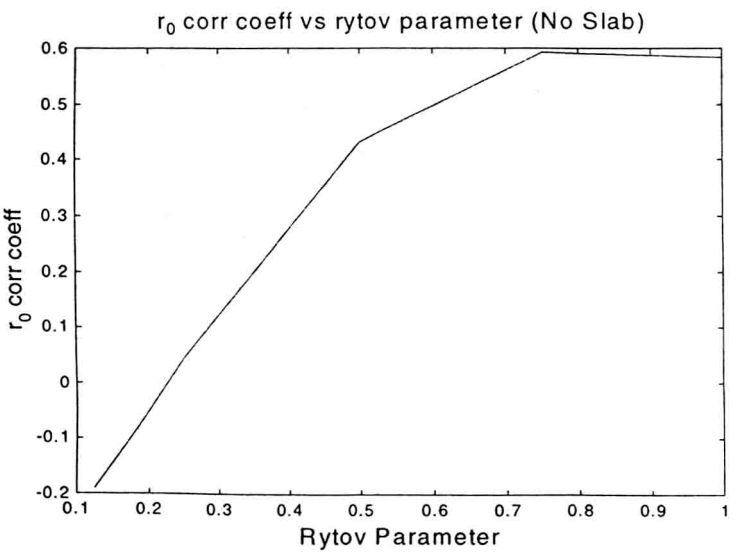

Figure 8: Correlation coefficient for PIB and r_0 vs. Rytov.

We did similar comparisons for θ_0 where similar, though weaker, correlations were observed. Since these were point source results, one might assume that θ_0 would not carry much information. However, due to the nature of the Rytov constraint, r_0 and θ_0 are correlated, as shown in Figure 9. The explanation is that, for a fixed Rytov, if we have a small r_0 then θ_0 must be large. This is because if the turbulence is concentrated in the near field, i.e. small r_0, then it cannot also be concentrated in the far field, i.e. small θ_0, and still maintain the Rytov value.

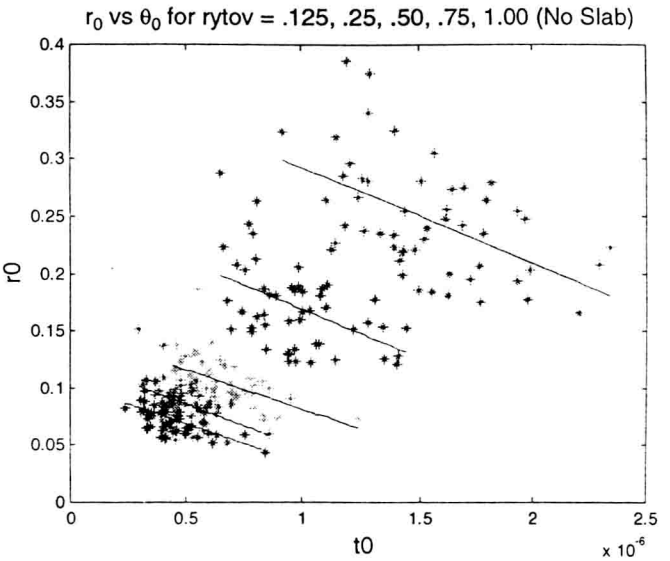

Figure 9 – Scatter plot for PIB vs. θ_0. The straight lines are regression lines for the different Rytov values.

4. FUTURE PLANS

In the future we plan to extend this study to include extended beacons, where θ_0 will be expected to play a key role. We also plan to increase the statistical base in order to create a performance estimator based on knowledge of Rytov or one of it's proxies – intensity variance or slope discrepancy – and of r_0 and θ_0.

5. ACKNOWLEGEMENTS

The Air Force Office of Scientific Research under AFRL Laboratory Task LRIR: 93PL001 supported this work.

6. REFERENCES

1. M. Roggemann and B. Welsh, "Imaging Through Turbulence", CRC Press, 1996.

Rytov parameter estimation by use of differential-tilt measurements

Matthew R. Whiteley

Airborne Laser Technology Branch, Air Force Research Laboratory,
3550 Aberdeen Avenue SE, Kirtland Air Force Base, New Mexico 87117-5776

ABSTRACT

The 'Rytov parameter' is a common name given to the log-amplitude variance predicted by an approximate solution to Maxwell's equations for propagation through media with random index of refraction (Rytov theory). Empirical evidence suggests that the Rytov parameter is a non-observable in many practical experiments where the variance of irradiance saturates, an effect not predicted by the standard theory. Nevertheless, the Rytov parameter is useful as an indicator of integrated turbulence strength for extended propagation and thus a desirable experimental quantity to estimate. In this work, we propose an optical configuration and related analysis techniques that provide a practical method for determining the Rytov parameter when scintillometry-based methods fail. This method employs differential-tilt measurements, resulting in a measurable quantity which is proportional to the Rytov parameter and for which Rytov theory is a good approximation. The differential-tilt technique is also insensitive to gimbal motion and additive noise. We illustrate that this method provides approximately 5% relative error in determining the Rytov parameter and may be used to characterize atmospheric turbulence well beyond the limits of conventional scintillometry.

Keywords: scintillation, differential tilt, Rytov theory

1 INTRODUCTION

The Rytov approximation is the predominant theoretical construct used to derive a solution to the scalar wave equation for propagation through a medium with random index-of-refraction fluctuations [1, 2]. Analysis of turbulence effects using the Rytov approximation is often referred to as 'Rytov theory.' The variance of the log-amplitude computed using Rytov theory is called the 'Rytov parameter.' This quantity is designated σ_χ^2 and is related to point-source propagation parameters as follows [2]:

$$\sigma_\chi^2 \equiv 0.5631 \left(\frac{2\pi}{\lambda}\right)^{7/6} \int_0^L \mathrm{d}z\, C_n^2(z)[z(1-z/L)]^{5/6}, \tag{1}$$

where λ is the wavelength, L is the propagation distance, z is a position along the propagation path, and C_n^2 is the index-of-refraction structure constant.

Eq. (1) indicates that σ_χ^2 should increase proportionately with any constant multiplier of C_n^2. However, experimental and simulation-based studies have concluded that Eq. (1) does not hold for full-wave propagation [3, 4, 5]. Instead, the irradiance variance (scintillation) increases monotonically from 0 to a maximum value greater than 1, then decreases as C_n^2 increases. This trend is referred to as the 'saturation' of scintillation. Saturation imposes a limit on the utility of irradiance-based instrumentation (scintillometers) to accurately determine integrated turbulence strength parameters using Rytov theory. In fact, in many experiments, the Rytov parameter cannot be measured directly, but rather must be inferred from measurable quantities making key assumptions about the turbulence profile that are not generally valid.

Propagation and Imaging through the Atmosphere IV, Michael C. Roggemann, Editor,
Proceedings of SPIE Vol. 4125 (2000) © 2000 SPIE · 0277-786X/00/$15.00

Despite its questionable relevance, the Rytov parameter is often used to quantify the severity of turbulence effects in propagation, especially in studies of scintillation phenomena [6]. Moreover, the Rytov parameter is a critical metric in determining the utility of adaptive-optical systems for compensation of extended-turbulence effects [7, 8]. Thus, it is often desirable to accurately estimate the Rytov parameter in field experiments where little or nothing is known about $C_n^2(z)$. For simulation studies, the Rytov parameter may be computed directly from the input parameters. An accurate estimate of the Rytov parameter in practical experiments therefore facilitates comparison with simulation-based studies.

To mitigate the difficulties associated with Rytov parameter estimation using irradiance measurements, we instead employ phase-related quantities for which Rytov theory is a reasonable model [9]. We have developed a novel method for obtaining a quantity that is proportional to the Rytov parameter using differential-tilt measurements. This technique is referred to as the *difference of differential-tilt variance* (DDTV). The analysis motivating and supporting the DDTV technique is described here in detail. It is important to clarify that the DDTV technique is used to estimate the value of the integral expression for σ_χ^2 given in Eq. (1), not the actual log-amplitude variance for point-source propagation. For certain configurations of the proposed optical apparatus, the relative error in the Rytov parameter estimate is approximately 0.05. The DDTV technique described here is insensitive to gimbal motion and additive detector noise, and is thought to be insensitive to turbulence outer scale and immune to saturation effects. The key advantage to this technique for Rytov parameter estimation over irradiance-based techniques is that differential-tilt measurements do not saturate, and may be analyzed accurately using Rytov theory.

The remainder of this paper is structured as follows. In Section 2, we present the theory and analysis associated with the DDTV method. The relationship between the DDTV measurement and the Rytov parameter is derived, and the criterion for estimator accuracy is established. In Section 3, we illustrate that reasonable optical configurations satisfy the basic requirements for Rytov parameter estimation. Also, we quantity the relative errors associated with this configuration. Furthermore, we quantify the magnitude of the expected measurements, indicating the scaling relationships for improving sensitivity. The research is summarized in Section 4.

2 THEORY AND ANALYSIS

We begin our analysis of the Rytov parameter estimation technique by considering a measurement model for tilt measurements made on two clear apertures, which we refer to as *aperture 1* and *aperture 2*. These apertures are used to observe either a single point source or two individual point sources, depending upon the measurement being considered. The technique described here requires measurements from both configurations, as shown in Figure 1. When both apertures observe a single point source, the configuration is referred to as *converging*. When the apertures observe separate point sources (source 1 and source 2), the configuration is referred to as *non-converging*. In practice, the single source for the 'converging' geometry may be either source 1 or source 2 (no need for a third source). Thus, the converging and non-converging configurations are obtained with the same apparatus. In general, each aperture observes both sources, and the distinction between converging and non-converging is made in processing the tilt data associated with each image of the point sources.

The Rytov estimation technique described here requires a measurement of the difference between the differential-tilt variance for the non-converging geometry and the differential-tilt variance for the converging geometry. This quantity is referred to as the difference of differential tilt variance (DDTV), is designated σ_δ^2, and is defined explicitly as:

$$\sigma_\delta^2 \equiv \left\langle (d_{1p} - d_{2p})^2 \right\rangle - \left\langle (d_{1c} - d_{2c})^2 \right\rangle , \tag{2}$$

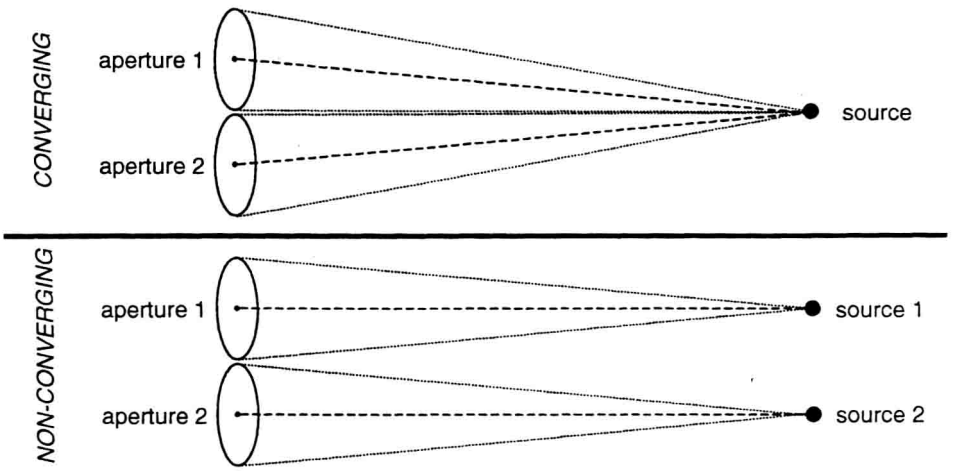

Figure 1: Schematic diagram of the two optical configurations required for Rytov parameter estimation from differential-tilt measurements. In practice, the single source for the 'converging' geometry may be either source 1 or source 2. Thus, the 'converging' and 'non-converging' geometries can be achieved with the same apparatus.

where d_{1p}, d_{2p} are tilt data from aperture 1, aperture 2, respectively for the non-converging configuration, d_{1c}, d_{2c} are tilt data from aperture 1, aperture 2, respectively for the converging configuration, and $\langle\cdot\rangle$ indicates the statistical expectation operation over an ensemble of turbulence realizations (a time history for ergodic turbulence assumptions). In the definition of Eq. (2), we have implicitly assumed that $\langle d_{1p}\rangle = \langle d_{2p}\rangle$ and $\langle d_{1c}\rangle = \langle d_{2c}\rangle$. Thus, any bias between the mean tilt of aperture 1 and the mean tilt of aperture 2 must be subtracted before applying Eq. (2) directly. It is worth noting here that Eq. (2) is a scalar equation to be applied to each component of the measured tilt vector. The analysis which follows will be carried out in a single axis of tilt, but the results are applicable to either axis.

At this point, the relation between σ_δ^2 and the Rytov parameter σ_χ^2 is ambiguous. The appropriate relationship becomes apparent only after considering how σ_δ^2 relates to propagation and turbulence parameters. To motivate this analysis, we consider a measurement model for tilt data from each aperture with non-converging and converging propagation paths. In this measurement model, we express each tilt measurement as the sum three components; atmospheric, noise, and gimbal motion. Accordingly, the tilt data from each aperture is given by:

$$\begin{aligned} d_{1p} &= t_{1p} + n_{1p} + \theta_p, \\ d_{2p} &= t_{2p} + n_{2p} + \theta_p, \\ d_{1c} &= t_{1c} + n_{1c} + \theta_c, \\ d_{2c} &= t_{2c} + n_{2c} + \theta_c. \end{aligned} \tag{3}$$

In Eq. (3), t_{1p}, t_{2p} and t_{1c}, t_{2c} represent atmospheric tilt components of the measured data from each aperture for the non-converging (p) and converging (c) propagation geometries. Also, n_{1p}, n_{1c} and n_{2p}, n_{2c} represent the detector-noise-induced angle for each aperture in the two geometries. The contribution of gimbal motion to the measured tilt on each aperture is given by θ_p and θ_c, indicating that aperture 1 and aperture 2 are mounted on the same gimbal (gimbal motion contributes the same tilt to each aperture).

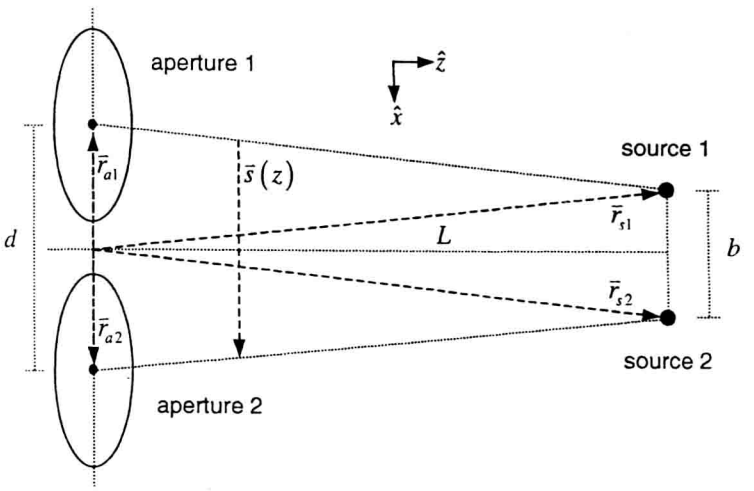

Figure 2: Analysis geometry for calculating the tilt covariance between apertures separated by a distance d in the $\hat{x}$ direction for point sources separated by a distance b in the $\hat{x}$ direction.

From the definition of σ_δ^2 in Eq. (2) and the model for the tilt data given in Eq. (3) it follows that:

$$\begin{aligned}
\sigma_\delta^2 &= \left\langle (t_{1p} - t_{2p} + n_{1p} - n_{2p})^2 \right\rangle - \left\langle (t_{1c} - t_{2c} + n_{1c} - n_{2c})^2 \right\rangle \\
&= \left\langle t_{1p}^2 \right\rangle + \left\langle t_{2p}^2 \right\rangle - 2\left\langle t_{1p} t_{2p} \right\rangle + \left\langle n_{1p}^2 \right\rangle + \left\langle n_{2p}^2 \right\rangle - 2\left\langle n_{1p} n_{2p} \right\rangle \\
&\quad - \left\langle t_{1c}^2 \right\rangle - \left\langle t_{2c}^2 \right\rangle + 2\left\langle t_{1c} t_{2c} \right\rangle - \left\langle n_{1c}^2 \right\rangle - \left\langle n_{2c}^2 \right\rangle + 2\left\langle n_{1c} n_{2c} \right\rangle \\
&= 2\left(\left\langle t_{1c} t_{2c} \right\rangle - \left\langle t_{1p} t_{2p} \right\rangle \right). \qquad (4)
\end{aligned}$$

In the steps leading up to Eq. (4), the noise variances and covariances are assumed to be equal for the converging and non-converging geometries. We also assume that n_{1p}, n_{2p} are uncorrelated with t_{1p}, t_{2p} and n_{1c}, n_{2c} are uncorrelated with t_{1c}, t_{2c}. Notice that the gimbal-motion contributions are canceled by the differencing of the tilt measurements for the common-gimbal apertures. Furthermore, the atmospheric tilt variances as well as the noise variances and covariances are canceled by the differencing of the differential-tilt variances. All that remains in the expression for σ_δ^2 is the difference of atmospheric tilt covariances for the converging and non-converging propagation geometries. Thus, σ_δ^2 is insensitive to contamination from gimbal motion and any additive noise source.

According to Eq. (4), σ_δ^2 represents twice the difference of tilt covariance between the two apertures for the converging and non-converging propagation geometries, as shown in Figure 1. To relate σ_δ^2 to the Rytov parameter, we must first consider the relation between the tilt covariance and turbulence parameters for each configuration. This calculation has been performed previously for Zernike coefficients of arbitrary order, with arbitrarily-positioned apertures and sources [10, 11, 12]. To employ the results of these analyses here, we consider the analysis geometry shown in Figure 2. This figure shows two apertures separated by a distance d in the $\hat{x}$ direction. These apertures are used to observe two point sources separated by a distance b in the $\hat{x}$ direction. This geometry is general enough to model both the converging and non-converging configurations ($b = 0$ for the converging geometry).

For two apertures (diameter D) separated in the $\hat{x}$ direction assuming a finite outer scale for turbulence L_0, the covariance of the Zernike x-tilt coefficients for the two apertures, designated a_1 and a_2 is given

by [10]:

$$\langle a_1 a_2 \rangle = 2^{1/3}\sqrt{3}\,\Gamma(8/3)\left(\frac{2\pi}{\lambda}\right)^2 D^{5/3}\int_0^L \mathrm{d}z\; C_n^2(z)(1-z/L)^{-2} \times \int_0^\infty \frac{\mathrm{d}x}{x}(x^2+x_0^2)^{-11/6} J_2^2[(1-z/L)x]\left\{J_0\left[\frac{2s(z)}{D}x\right] - J_2\left[\frac{2s(z)}{D}x\right]\right\}, \quad (5)$$

where λ is the wavelength, L is the propagation distance, C_n^2 is the index of refraction structure constant, $x_0 = \pi D/L_0$, and $s(z)$ is the magnitude of $\vec{s}(z)$ shown in Figure 2:

$$\vec{s}(z) = (1-z/L)(\vec{r}_{a_2} - \vec{r}_{a_1}) + (z/L)(\vec{r}_{s_2} - \vec{r}_{s_1}), \quad (6)$$

$$s(z) = d(1-z/L) + b(z/L). \quad (7)$$

Notice that since the aperture and source separations are in the $\hat{x}$ direction, $\vec{s}(z)$ is always parallel to $\hat{x}$.

The physical configurations we wish to consider involve small separations of the apertures and sources. In these cases, outer scale effects will be negligible. Thus, for $x_0 \to 0$, Eq. (5) may be written as:

$$\langle a_1 a_2 \rangle = 16\sqrt{3}\,\Gamma(8/3)\left(\frac{2\pi}{\lambda}\right)^2 D^{5/3} L\int_0^1 \mathrm{d}\xi\; C_n^2(\xi L)\,\frac{[\alpha(\xi)]^{11/3}}{(1-\xi)^{-2}}\int_0^\infty \frac{\mathrm{d}\gamma}{\gamma}\gamma^{-11/3} J_2^2[\beta(\xi)\gamma]\Big\{J_0(\gamma) - J_2(\gamma)\Big\}, \quad (8)$$

where $\xi = z/L$ and $\alpha(\xi)$, $\beta(\xi)$ are dimensionless parameters given by:

$$\alpha(\xi) = \frac{s(\xi)}{D}, \quad (9)$$

$$\beta(\xi) = \frac{1-\xi}{2\alpha(\xi)}. \quad (10)$$

From Eq. (7) and Eq. (9) we note that $\langle a_1 a_2 \rangle$ for a given $C_n^2(z)$ depends only upon the normalized aperture separation d/D and the normalized source separation b/D. If we treat all factors multiplying C_n^2 within the integral over ξ as a weighting function $W(\xi)$, then Eq. (8) may be rewritten as:

$$\langle a_1 a_2 \rangle = 16\sqrt{3}\,\Gamma(8/3)\left(\frac{2\pi}{\lambda}\right)^2 D^{5/3} L\int_0^1 \mathrm{d}\xi\; C_n^2(\xi L)\; W(\xi), \quad (11)$$

where $W(\xi)$ is defined as:

$$W(\xi) \equiv \frac{[\alpha(\xi)]^{11/3}}{(1-\xi)^{-2}}\int_0^\infty \frac{\mathrm{d}\gamma}{\gamma}\gamma^{-11/3} J_2^2[\beta(\xi)\gamma]\Big\{J_0(\gamma) - J_2(\gamma)\Big\}. \quad (12)$$

The integral over γ may be evaluated in closed form. The value of the integral depends upon the value of the parameter $\beta(\xi)$ as follows:

For $[\beta(\xi)]^2 < 1/4$:

$$W(\xi) = 2^{-14/3}(1-\xi)^{5/3}\left[\begin{array}{l} 2^{-17/3}[\beta(\xi)]^{1/3}\dfrac{\Gamma(1/6)}{\Gamma(5/6)}\,{}_3F_2\left\{1/6, 1/6, 5/2; 3, 5; [2\beta(\xi)]^2\right\} \\ \\ -2^{-17/3}[\beta(\xi)]^{1/3}\dfrac{\Gamma(7/6)}{\Gamma(11/6)}\,{}_3F_2\left\{-5/6, 7/6, 5/2; 3, 5; [2\beta(\xi)]^2\right\} \end{array}\right] \quad (13)$$